Support Information

Underestimated benefits of NO_x control in reducing SNA and O_3 based on missing heterogeneous HONO sources

Shuping, Zhang[1,2,3], Haotian Zheng[1], Jun Liu[3], Yao Shi[1], Tianzeng Chen[3], Chaoyang Xue[3], Fenfen Zhang[1], Yueqi Jiang[1], Xiangping Zhang[4], Shovan Kumar Sahu[5], Biwu Chu[3]*, Jia Xing[1]*,

[1]State Key Joint Laboratory of Environment Simulation and Pollution Control, School of Environment, Tsinghua University, Beijing 100084, China

[2]China Academy of Civil Aviation Science and Technology, Beijing 100028, China

[3]State Key Joint Laboratory of Environment Simulation and Pollution Control, Research Center for Eco-Environmental Sciences, Chinese Academy of Sciences, Beijing 100085, China

[4]Yellow River Institute of Hydraulic Research, Zhengzhou 450003, China

[5]Centre for Climate Research Singapore, Meteorological Service Singapore, Singapore 537054, Singapore

Correspondence to: Jia Xing(xingj02@gmail.com), Biwu Chu (bwchu@rcees.ac.cn)

The analysis of formation process of O_3

Owing to short life span of OH radicals, the concentration of OH only affected by CHEM process (Figure S4). For surface-level O_3, VDIF is the major source and DDEP and CHEM are the major sink. The average of the chemical IPRs was approximately -35.4μg/m^3/h and -38.6μg/m^3/h in REV and ORI, respectively. VDIF enhanced O_3 rate from 29.8 μgm^{-3}/h to 34.5μg/m^3/h. The results means that O_3 in surface layer mainly came from upper layers by vertical turbulent mixing while chemical process in surface layer consumed O_3.

Table S1 A comparison of WRF simulated and observed with observed temperature, wind speed, and water vapor mixing ratio in China

	WS (m/s)	T(℃）	H(g/kg)	WD (°)
Bias	0.04	-0.98	-0.91	3.87
Gross Error	1.08	1.94	1.79	50.57
RMSE	1.47	2.62	2.29	
IOA	0.78	0.96	0.94	

Table S2 Heterogeneous HONO reactions used in this study

Reaction No.	Reaction	Reaction Rate Constant (k)	Uptake coefficient (γ)	Reference
1a.	NO_2 + aerosol = 0.5×HONO + 0.5×HNO_3	$k = \frac{1}{4}\gamma v_{NO2}\frac{S}{V_a}$	$\gamma_{an} = 8\times10^{-6}$	(Liu et al., 2019)
1b.	NO_2 + aerosol + hv = 0.5×HONO + 0.5×HNO_3	$k = \frac{1}{4}\gamma v_{NO2}\frac{S}{V_a}\times\frac{J}{J_{max}}$	$\gamma_{ad} = 1\times10^{-3}$	(Liu et al., 2019)
2a.	NO_2 + ground = HONO	$k=\frac{1}{8}\gamma v_{NO2}\frac{1.7}{H}$	$\gamma_{gn} = 2\times10^{-6}$	(Li et al., 2018; Liu et al., 2019)
2b.	NO_2 + ground + hv = HONO	$k=\frac{1}{8}\gamma v_{NO2}\frac{1.7}{H}\times\frac{J}{J_{max}}$	$\gamma_{gd} = 6\times10^{-5}$	(Liu et al., 2019)
3	NO_3^- + hv = 0.67×HONO + 0.33×NO_2	$J = 30\times J_{HNO3}$		(Romer et al., 2018)
4	NO_2 + EC= 0.61×HONO + 0.39×NO	$k = \frac{1}{4}\gamma v_{NO2}\frac{S\_BET}{V}$	$\gamma = 2\times10^{-6}$	(Spataro and Ianniello, 2014)
5	HNO_3 + $NaNO_2$ (s) = HONO + $NaNO_3$ (s)	$k=0.06V_{dep\_HNO3}/H$		(VandenBoer et al., 2015)
6	HCl + $NaNO_2$ (s) = HONO + NaCl (s)	$k=0.2V_{dep\_HCl}/H$		(VandenBoer et al., 2015)

Note:

k is the first order rate constant in seconds per second (1/sec), γ is the heterogeneous uptake coefficient, γ_{an} is the night-time heterogeneous uptake coefficient on aerosol, γ_{ad} is the day-time heterogeneous uptake coefficient on aerosol, γ_{gn} is the night-time heterogeneous uptake coefficient on ground, γ_{gd} is the day-time heterogeneous uptake coefficient on ground, S/V_a is the density of aerosol surface, S/V_g is the density of ground surface, v is the mean molecular speed in meters per second (m/s), HNO_3 is nitric acid, $NaNO_2$ is sodium nitrite, NaCl is sodium chloride, J is the NO_2 photolysis rate coefficient, J_{max} is the maximum NO_2 photolysis rate coefficient, V_{dep_HNO3} is the deposition velocity of HNO_3 in meters per second (m/s), V_{HCl} is the deposition velocity of HCl in meters per second (m/s), H is the first-layer height in meters(m), and S_BET/V is the BET surface area-to-volume ratio calculated as CMAQv5.3 predicted elemental carbon (EC) ($\mu g/m^3$) × 1.0 ×10^{-6} (g/μg) ×122 m^2/g. Reactions 1a, 1b, 2a, and 2b were revised from CMAQv5.3, while reactions 3, 4, 5, and 6 are newly added reactions.

Table S3: Average VOC concentrations and reaction rates of VOCS with OH in the ORI and REV models in Beijing

	Conc (μg/m³)		R_{VOC+OH} (ng/m³/h)		MIR	OFP	
	ORI	REV	ORE	REV		ORI	REV
Acetaldehyde	2.21	2.30	0.16	0.19	4.45	5.01	5.22
Higher-aldehydes	7.97	8.01	0.24	0.28	6.81	13.50	13.57
Ethene	4.25	4.19	0.05	0.06	4.37	14.82	14.62
Ethane	2.61	2.60	0.00	0.00	0.11	0.21	0.21
Ethanol	3.06	3.02	0.03	0.03	1.04	1.55	1.53
Formaldehyde	3.60	3.75	0.21	0.25	4.50	12.07	12.57
Internal olefin	2.66	2.50	0.06	0.07	13.11	6.30	5.92
Isoprene	1.09	0.95	0.61	0.69	11.56	4.14	3.59
Methanol	2.11	2.07	0.01	0.02	0.36	0.53	0.52
Olefin	14.65	14.25	0.39	0.46	8.24	21.77	21.17
Paraffin	1351.47	1342.37	2.22	2.61	0.32	28.38	28.18
Monoterpenes	1.30	0.82	0.21	0.17	8.82	0.48	0.30
Toluene	17.58	17.41	0.16	0.19	2.94	12.57	12.45
Xylene	16.20	15.93	0.33	0.39	14.79	50.57	49.72

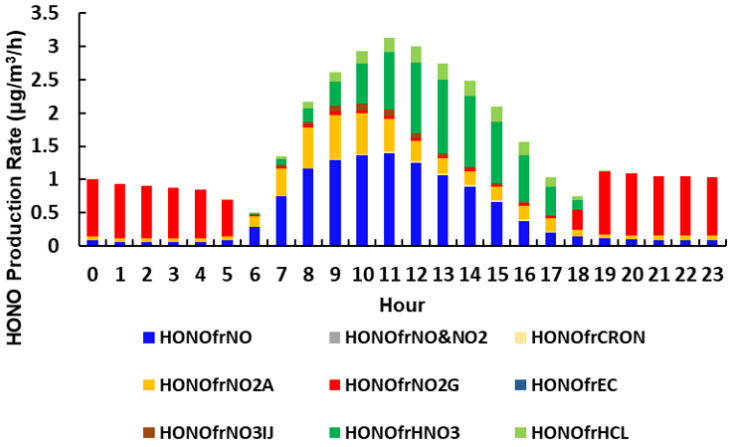

Figure S1 Production rates of different HONO reactions to near-ground-level HONO concentration in Beijing in summer. The production from the NO+OH reaction is denoted as HONOfrNO, the production from the $NO+NO_2+H_2O$ reaction is denoted as HONOfrNO&NO2, the production from cresol is denoted as HONOfrCRON, the production from the heterogeneous reaction on ground surfaces is denoted as HONOfrNO2G, the production from the heterogeneous reaction on aerosol surfaces is denoted as HONOfrNO2A, the production from the reaction of EC is denoted as HONOfrEC, the production from the photolysis of NO_3^- is denoted as HONOfrNO3IJ, the production from the acid displacement reaction of HNO_3 is denoted as HONOfrHNO3, and the production from acid displacement reaction of HCl is denoted as HONOfrHCL.

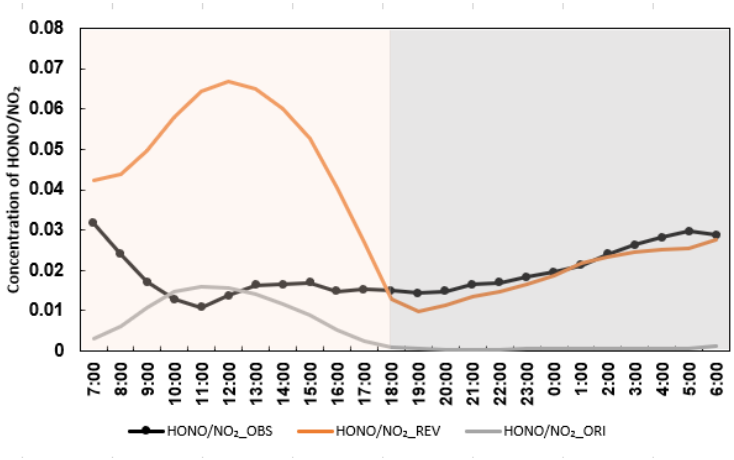

Figure S2 Average diurnal variation of $HONO/NO_2$ during August 16 to September 15, 2018 in Beijing

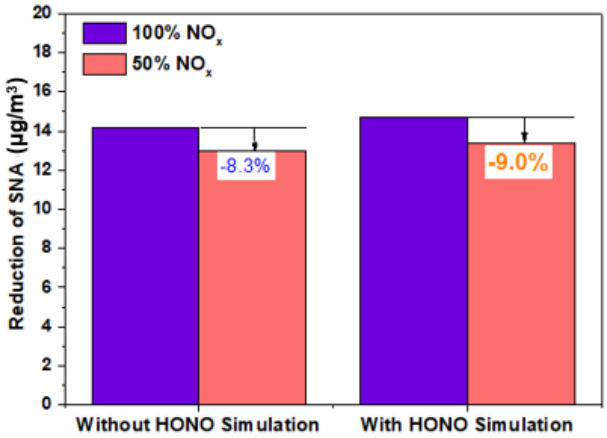

Figure S3 Changes of SNA concentration in the presence and absence of HONO heterogeneous reactions with 50% NO_x reductions in 2018.

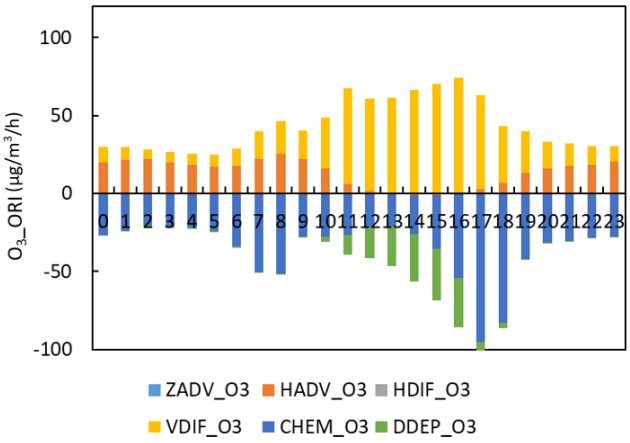

Figure S4 The changes of O_3 concentration from different process with the ORI case. The change of O_3 concentration from vertical advection is denoted as ZADV_O3, The change of O_3 concentration from horizontal advection is denoted as HADV_O3, The change of O_3 concentration from horizontal diffusion is denoted as HDIF_O3, The change of O_3 concentration from vertical diffusion is denoted as VDIF_O3, The change of O_3 concentration from gas-phase chemistry is denoted as CHEM_O3, The change of O_3 concentration from dry deposition is denoted as DDEP_O3,

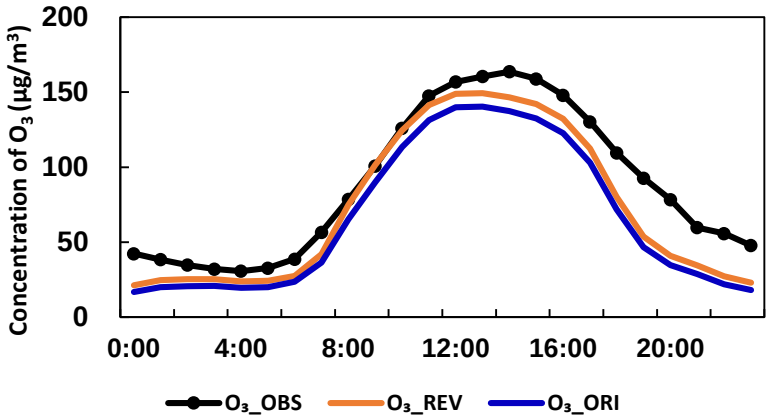

Figure S5 Average diurnal variation of O_3 during August 16 to September 15, 2018 in Beijing

Table S4 Response of the 90th percentile of MDA8 O_3 to NOx emission reduction in different percentage

NOx Emission Reduction	90%-MDA8 O_3 ($\mu g\ m^{-3}$)		△90%-MDA8 O_3 ($\mu g\ m^{-3}$)		△90%-MDA8 O_3 Reduction Percentage	
	ORI	REV	ORI	REV	ORI	REV
100%	141.9	157.5				
80%	135.2	149.4	-6.7	-8.1	-4.7%	-5.2%
50%	137.8	152.8	-4.1	-4.7	-2.9%	-3.0%
20%	140.6	153.9	-1.3	-3.6	-0.9%	-2.3%

References

Li D D, Xue L K, Wen L, Wang X F, Chen T S, Mellouki A, Chen J M, Wang W X (2018). Characteristics and sources of nitrous acid in an urban atmosphere of northern China: Results from 1-yr continuous observations. Atmospheric Environment, 182: 296-306

Liu Y, Lu K, Li X, Dong H, Tan Z, Wang H, Zou Q, Wu Y, Zeng L, Hu M, Min K-E, Kecorius S, Wiedensohler A, Zhang Y (2019). A Comprehensive Model Test of the HONO Sources Constrained to Field Measurements at Rural North China Plain. Environmental Science & Technology, 53(7): 3517-3525

Romer P S, Wooldridge P J, Crounse J D, Kim M J, Wennberg P O, Dibb J E, Scheuer E, Blake D R, Meinardi S, Brosius A L, Thames A B, Miller D O, Brune W H, Hall S R, Ryerson T B, Cohen R C (2018). Constraints on Aerosol Nitrate Photolysis as a Potential Source of HONO and NOx. Environmental Science & Technology, 52(23): 13738-13746

Spataro F, Ianniello A (2014). Sources of atmospheric nitrous acid: State of the science, current research needs, and future prospects. Journal of the Air & Waste Management Association, 64(11): 1232-1250

Vandenboer T C, Young C J, Talukdar R K, Markovic M Z, Brown S S, Roberts J M, Murphy J G (2015). Nocturnal loss and daytime source of nitrous acid through reactive uptake and displacement. Nature Geoscience, 8(1): 55-60